BJP British Journal of Pharmacology

DOI:10.1111/bph.12521
www.brjpharmacol.org

RESEARCH PAPER

Structural requirements of steroidal agonists of transient receptor potential melastatin 3 (TRPM3) cation channels

A Drews[1,*,†], F Mohr[2,*], O Rizun[2], T F J Wagner[1,‡], S Dembla[1,2], S Rudolph[1], S Lambert[1], M Konrad[2], S E Philipp[1], M Behrendt[2], S Marchais-Oberwinkler[3], D F Covey[4] and J Oberwinkler[2]

[1]*Experimentelle und Klinische Pharmakologie und Toxikologie, Universität des Saarlandes, Homburg, Germany,* [2]*Institut für Physiologie und Pathophysiologie, Philipps-Universität Marburg, Marburg, Germany,* [3]*Institut für Pharmazeutische Chemie, Philipps-Universität Marburg, Marburg, Germany, and* [4]*Department of Developmental Biology, School of Medicine, Washington University in St. Louis, St. Louis, MO, USA*

Correspondence
Johannes Oberwinkler, Institut für Physiologie und Pathophysiologie, Philipps-Universität Marburg, Deutschhausstr. 1-2, 35037 Marburg, Germany. E-mail: johannes.oberwinkler@uni-marburg.de

*These authors contributed equally to this work.

Present address: †Department of Chemistry, Cambridge University, Cambridge, UK. ‡Department of Cell Biology and Dorris Neuroscience Center, The Scripps Research Institute, La Jolla, CA, USA.

Keywords
cation membrane channel; ClC-3; dihydropyridine; enantiomer; neurosteroid; pregnenolone sulphate; proton-activated outwardly rectifying anion channel; PAORAC; transient receptor potential; transient receptor potential melastatin

Received
5 September 2013
Revised
29 October 2013
Accepted
13 November 2013

BACKGROUND AND PURPOSE
Transient receptor potential melastatin 3 (TRPM3) proteins form non-selective but calcium-permeable membrane channels, rapidly activated by extracellular application of the steroid pregnenolone sulphate and the dihydropyridine nifedipine. Our aim was to characterize the steroid binding site by analysing the structural chemical requirements for TRPM3 activation.

EXPERIMENTAL APPROACH
Whole-cell patch-clamp recordings and measurements of intracellular calcium concentrations were performed on HEK293 cells transfected with TRPM3 (or untransfected controls) during superfusion with pharmacological substances.

KEY RESULTS
Pregnenolone sulphate and nifedipine activated TRPM3 channels supra-additively over a wide concentration range. Other dihydropyridines inhibited TRPM3 channels. The natural enantiomer of pregnenolone sulphate was more efficient in activating TRPM3 channels than its synthetic mirror image. However, both enantiomers exerted very similar inhibitory effects on proton-activated outwardly rectifying anion channels. Epiallopregnanolone sulphate activated TRPM3 almost equally as well as pregnenolone sulphate. Exchanging the sulphate for other chemical moieties showed that a negative charge at this position is required for activating TRPM3 channels.

© 2013 The Authors. British Journal of Pharmacology published by John Wiley & Sons Ltd on behalf of The British Pharmacological Society.
This is an open access article under the terms of the Creative Commons Attribution-NonCommercial License, which permits use, distribution and reproduction in any medium, provided the original work is properly cited and is not used for commercial purposes.

CONCLUSIONS AND IMPLICATIONS

Our data demonstrate that nifedipine and pregnenolone sulphate act at different binding sites when activating TRPM3. The latter activates TRPM3 by binding to a chiral and thus proteinaceous binding site, as inferred from the differential effects of the enantiomers. The double bond between position C5 and C6 of pregnenolone sulphate is not strictly necessary for the activation of TRPM3 channels, but a negative charge at position C3 of the steroid is highly important. These results provide a solid basis for understanding mechanistically the rapid chemical activation of TRPM3 channels.

Abbreviations

PAORAC, proton-activated outwardly rectifying anion channel; PS, pregnenolone sulphate; TRP, transient receptor potential; TRPM, transient receptor potential melastatin

Introduction

The regulation of ion channel activity by pharmacological means is a widely used strategy for therapeutic treatments as well as for experimental investigations. Its relevance is expected to increase substantially in the future (Bagal *et al.*, 2013). Often, several substances with dissimilar chemical structures act upon a single type of ion channel. In these cases, the simultaneous presence of two or more substances can have combined effects on channel activity that are not readily predicted from the responses to a single class of substance in isolation.

Many members of the transient receptor potential (TRP) ion channel family exemplify these points, as these proteins are often influenced by a bewildering variety of chemically highly diverse compounds (Moran *et al.*, 2011). This is also true for transient receptor potential melastatin 3 (TRPM3; the nomenclature in this paper follows BJP's Concise Guide to PHARMACOLOGY, Alexander *et al.*, 2013), one of the least studied members of this important class of ion channels (Oberwinkler and Philipp, 2007). Transcripts encoding for TRPM3 channels have been described in a variety of tissues and cell types (Grimm *et al.*, 2003; Lee *et al.*, 2003; Oberwinkler *et al.*, 2005; Fonfria *et al.*, 2006; Kunert-Keil *et al.*, 2006; Wagner *et al.*, 2008; Vriens *et al.*, 2011). However, in most of the TRPM3-expressing tissues, the function of these channels is not well understood. As an exception, there is strong evidence, obtained using knockout mice, that TRPM3 is involved in detecting noxious heat stimuli in a subset of dorsal root ganglion (DRG) neurons (Vriens *et al.*, 2011). This notion has since been strengthened using pharmacological approaches with TRPM3 antagonists (Straub *et al.*, 2013a,b). In addition, in beta cells of pancreatic islets, pharmacologically-activated TRPM3 channels have been found to enhance glucose-induced insulin secretion and the influx of Zn^{2+} ions (Wagner *et al.*, 2008; 2010; Klose *et al.*, 2011; Lambert *et al.*, 2011). Also, TRPM3 channels have been implicated in the enhancement of contraction and in suppression of cytokine secretion in vascular smooth muscle cells (Naylor *et al.*, 2010).

The identification and characterization of endogenously expressed TRPM3 channels in these cell types has heavily relied upon pharmacological approaches to activate TRPM3 channels. The first TRPM3 agonist described was D-erythro-sphingosine (Grimm *et al.*, 2005). Subsequently, the 1,4-dihydropyridine nifedipine and the steroid pregnenolone sulphate (PS) were identified as structurally different TRPM3 agonists (Wagner *et al.*, 2008). All three compounds are only moderately potent TRPM3 agonists, as the reported EC_{50} values are in the μM concentration range. Nevertheless, they still exhibit a reasonably narrow structure–activity relationship, because even minor modifications of the chemical structures strongly increase the apparent EC_{50} values or dramatically lower the response amplitude. This has been especially well demonstrated for steroidal compounds, as small chemical modifications of PS have been shown to reduce the effects of the resulting substances [such as pregnenolone, dehydroepiandrosterone (DHEA) or DHEA sulphate] on TRPM3 channels (Wagner *et al.*, 2008; Majeed *et al.*, 2010). Other steroidal substances with even more divergent structures have either been demonstrated to be inhibitory, for example, progesterone or cholesterol (Majeed *et al.*, 2010; Naylor *et al.*, 2010), or have no detectable effect, for example, oestrogens, glucocorticoids, allopregnanolone (Wagner *et al.*, 2008) and bile acids (Düfer *et al.*, 2012). However, Majeed *et al.* (2010) reported that epipregnanolone sulphate also activates TRPM3 channels rather strongly, although not as strongly as PS.

Equally, the specific structure of nifedipine seems to be important for activating TRPM3 channels, as other 1,4-dihydropyridines (nimodipine, nitrendipine and nicardipine) do not activate TRPM3 (Wagner *et al.*, 2008). This is in stark contrast to the situation seen with TRPA1 channels that are activated by all of these dihydropyridines (Fajardo *et al.*, 2008a,b). Similarly, structural analogues of D-erythro-sphingosine (e.g. dihydro-D-erythro-sphingosine, *N*,*N*-dimethyl-D-erythro-sphingosine or sphingosine-1-phosphate) were reported to have substantially less agonistic effect on TRPM3 channels than D-erythro-sphingosine itself (Grimm *et al.*, 2005). These, rather narrow, structure–activity relationships are somewhat surprising and indicate that further investigations are warranted to improve our understanding of agonist binding to TRPM3 channels. In particular, the multitude of structurally unrelated chemical activators for TRPM3 raises important questions about the nature of the binding site of these compounds, their mode of action and their potential interaction. We started to address these questions by studying how 1,4-dihydropyridine compounds interact with the agonistic action of PS on TRPM3 channels. We also investigated whether PS activates TRPM3 by directly binding to a protein moiety. In addition, we enhanced our understanding of the structural characteristics of steroids important for TRPM3 activation.

Methods

Cell culture and TRPM3 cDNA

HEK293 cells and HEK293 cells stably transfected with either myc-TRPM3α2-YFP (in Figure 6A and B and in Figure 7B and C and in parts of Figure 3D and E and Figure 6C) or myc-TRPM3α2 (unless otherwise mentioned in this section) were used as described previously (Wagner *et al*., 2010; Frühwald *et al*., 2012). Alternatively (for Figure 2C and D), we used HEK293 cells transiently transfected with TRPM3α2 as described in Wagner *et al*. (2008). Neither in this study, nor in our previous work, did we observe differences in the channel properties due to tags or transfection methods employed. All TRPM3 constructs used in this study were derived from murine (*Mus musculus*) clones (accession number: AJ544534). Cells were grown in minimal essential medium with 10% fetal calf serum. Geneticin (1%, Sigma-Aldrich Taufkirchen, Germany) was added to the medium for stably transfected cells. Cells were stored in a humidified atmosphere with 5% CO_2 at 37°C. Each cell line was passaged 2–3 times a week up to a passage number of 40. Even at this passage number, stably transfected cells vigorously responded to the application of PS. In addition, we verified the presence and integrity of the TRPM3 proteins expressed by Western blotting (Supporting Information Figure S1). For simplicity, we have used the term TRPM3 to designate the splice variant TRPM3α2 (Oberwinkler *et al*., 2005) for the remainder of the manuscript.

Chemical substances

ent-PS (the synthetic, unnatural enantiomer of PS) was synthesized as described previously (Nilsson *et al*., 1998). In this paper, we occasionally use the term *nat*-PS to refer to PS, in order to emphasize the difference from *ent*-PS. As reported in the original publication (Nilsson *et al*., 1998), the enantiomeric excess (ee) of this preparation was 97.2%, meaning that the sample contained 98.6% *ent*-PS and 1.4% *nat*-PS. All other steroids were obtained from Sigma-Aldrich or Steraloids (Newport, RI, USA). 1,4-Dihydropyridines were purchased from either Sigma-Aldrich or Biotrend (Köln, Germany). As a convenience for the reader, the structures of the dihydropyridines and steroids used are given in Supporting Information Tables S1 and 2. To obtain photo-inactivated nifedipine, 100 mM nifedipine dissolved in DMSO was illuminated with a UV-lamp (Uvico, Rapp OptoElectronic, Wedel, Germany) for 15 min.

Patch-clamp electrophysiology

For all measurements we used an extracellular solution containing (in mM) 145–150 NaCl, 10 CsCl, 3 KCl, 2 $CaCl_2$, 2 $MgCl_2$, 10 HEPES and 10 D-glucose (pH 7.2). To activate proton-activated outwardly rectifying anion channel (PAORAC) currents, we applied a solution containing (in mM) 145–150 NaCl, 10 CsCl, 3 KCl, 2 $CaCl_2$, 2 $MgCl_2$, 5 citric acid and 5 D-glucose (pH 4). In all solutions, the pH was adjusted with NaOH, and the concentrations indicated are the final values after adjustment of pH. Steroidal and dihydropyridine compounds were dissolved in DMSO to a stock concentration of 50 or 100 mM. The intracellular solution contained (in mM) 90 CsAsp, 45 CsCl, 10 BAPTA, 5 EDTA, 4 Na_2ATP and 10 HEPES (pH 7.2 with CsOH). We applied voltage ramps from –115 to +85 mV (1 mV·ms^{-1}) from a holding potential of -15 mV at a rate of 1 Hz and analysed the current amplitudes at –80 and +80 mV offline. The liquid junction potential was calculated to be 15 mV with Clampex 8.1 (Molecular Devices, Sunnyvale, CA, USA) and all potential values given are corrected to this value. Whole-cell capacitance was measured with an EPC-10 amplifier controlled by the Patchmaster software (HEKA Elektronik, Lambrecht/Pfalz, Germany) with the built-in slow capacitance and series-resistance compensation feature.

Calcium imaging

HEK293 cells stably expressing TRPM3 channels or untransfected HEK293 cells were cultured on poly-L-lysin coated glass coverslips. Cells were loaded in culture medium containing 5 μM Fura2-AM [from Mobitec (Göttingen, Germany) or Biotrend, prepared as a 1 mM stock in DMSO] for 30 min. Fura2 loaded cells were washed three times with the bath solution that was also used during the experiments and contained (in mM): 145 NaCl, 10 CsCl, 2–5 KCl, 2 $CaCl_2$, 2 $MgCl_2$, 10 HEPES, 10 D-glucose. pH was adjusted to 7.2 with NaOH. After being washed, cells were transferred to a closed recording chamber (Warner Instruments, Hamden, CT, USA) and constantly perfused at a rate of about 1 mL·min^{-1}. Stock solutions of steroids and 1,4-dihydropyridines used in imaging experiments were prepared either in water or DMSO. The final DMSO concentration never exceeded 0.2%. A Nikon TE2000 inverted microscope equipped with a 10× objective (SFluor; N.A. 0.5, Nikon, Düsseldorf, Germany) was used for all imaging experiments. Fluorescence at 510 nm was detected every 5 s with a Retiga-Exi camera (QImaging, Surrey, British Columbia, Canada) during excitation with light of 340 and 380 nm wavelength using a motorized filter wheel (Ludl, Hawthorne, NY, USA). Background fluorescence intensities were obtained and subtracted for each picture individually and ratio images 340/380 nm were subsequently calculated pixel by pixel with ImageJ (Abràmoff *et al*., 2004) using a modified version of the 'ratio plus' plug-in. Thresholding was used to limit the calculation of the ratio values to pixels with sufficient photon counts when stimulated with either of the two wavelengths.

For measuring the effects of cholesterol and methyl-β-cyclodextrin (Sigma-Aldrich), a different imaging set-up (TiLL-Photonics, Gräfelfing, Germany) based on a Zeiss Axiovert microscope was used, employing a Sensicam camera (PCO, Kehlheim, Germany) and TiLL-Vision software (TiLL-Photonics) for calculating the ratio values. The light source was a monochromator (Polychrome V, TiLL-Photonics) illuminated by a xenon arc lamp. With this set-up, pairs of fluorescence images were taken every 3 s.

Data analysis and statistics

Data were obtained from single cells and subsequently averaged. Time courses of Fura2 signals (ratio 340/380) are depicted as mean ± SEM. For statistical analyses of the calcium imaging experiments (Figures 6 and 7), the increase in the 340/380 nm ratio was evaluated 12 to 60 s after addition of the test compound relative to the baseline values before application of the substances. The values obtained were normalized to the average response to PS measured in the same cells. For the analysis of electrophysiological measurements, current amplitudes at –80 and +80 mV were read from the traces after current amplitudes had reached a stable plateau.

Baseline values obtained in the absence of agonists or antagonists were subtracted. Statistical significance was tested with two-tailed, paired Student's *t*-tests (Microsoft Excel), unless stated otherwise. In the figures, statistical significance is indicated by *, when $P < 0.01$, n.s. signifies 'not significant' ($P \geq 0.05$). The numerical values used for drawing the bar graphs, together with the number of cells analysed and the *P*-values obtained in statistical tests are given in Supporting Information Table S3. Hill curve fits (Figure 4C) were calculated with Graphpad Prism 3.0 (GraphPad Software, La Jolla, CA, USA).

Generation of the superimposed chemical structures

Structures for each compound were drawn and their energy minimized independently with Moe2010.10. Pairwise superimposition was performed using the manual fit method of Moe.

Results

Interactions between PS and nifedipine during TRPM3 activation

PS and nifedipine both activate TRPM3 channels strongly, quickly and reversibly (Wagner *et al.*, 2008). To test for possible interactions between these two agonists, we initially co-applied them during Fura2-based Ca^{2+}-imaging experiments (Figure 1A). The large and sustained increase in intracellular calcium induced by 50 μM PS was further increased by applying nifedipine (50 μM). Although PS and nifedipine have entirely different chemical structures, it is conceivable that both substances bind to the same or to overlapping binding sites. To investigate these questions further, we turned to patch-clamp electrophysiology, which allows a more direct and quantitative measurement of TRPM3 activation. Again, we found that co-applying PS and nifedipine

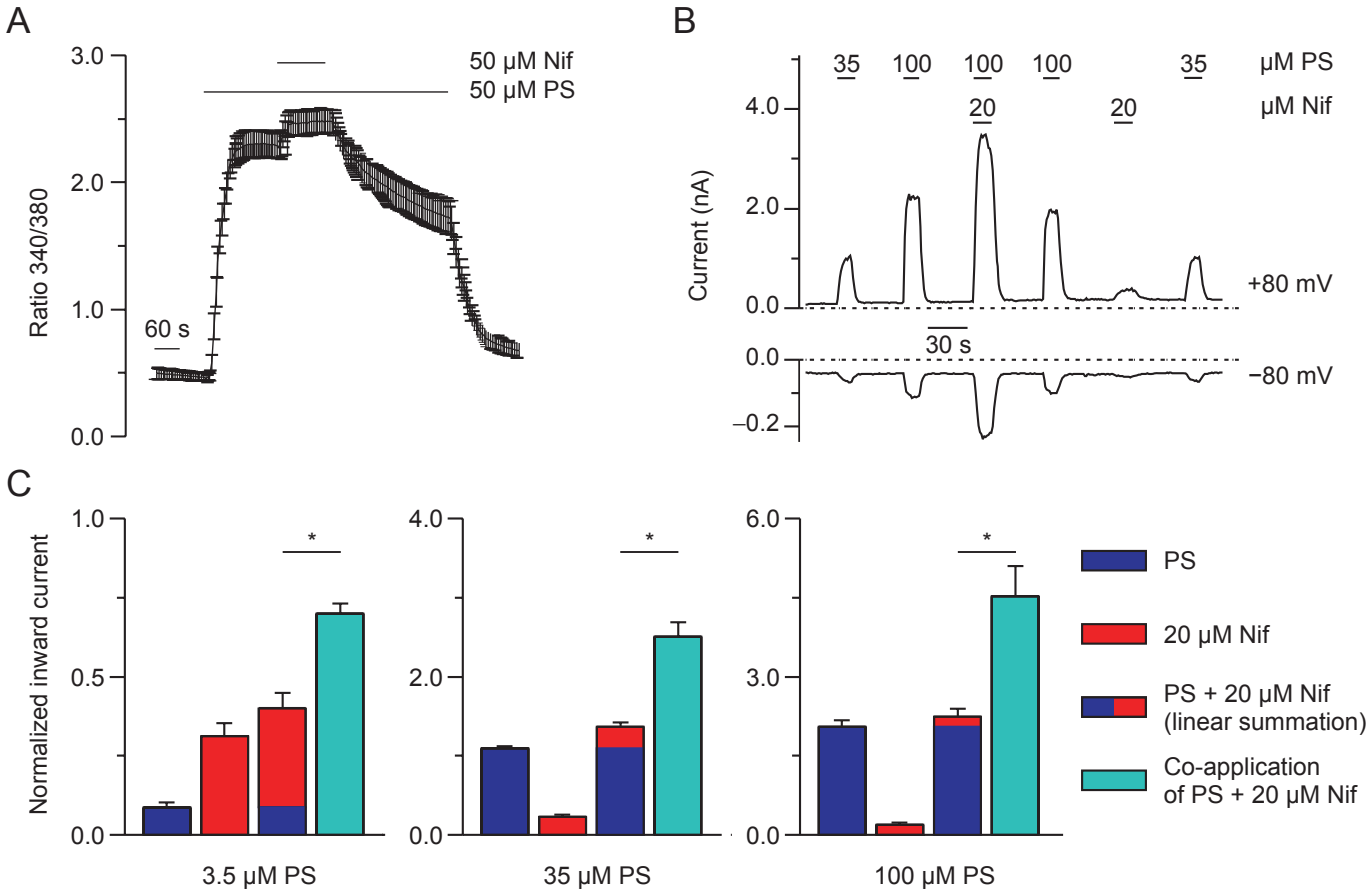

Figure 1

PS and nifedipine (Nif) activate TRPM3 channels supra-additively. (A) Ca^{2+}-imaging experiment with TRPM3-expressing cells stimulated with 50 μM PS, and 50 μM Nif together with 50 μM PS ($n = 20$). The addition of Nif increased the intracellular Ca^{2+}-concentration. (B) Representative whole-cell patch-clamp experiment during which PS and Nif (at indicated concentrations) were applied to a TRPM3-expressing cell. The current–voltage relationships observed during this recording were highly similar to the outwardly rectifying curves typical for TRPM3 currents published previously (Wagner *et al.*, 2008) and are depicted in Supporting Information Figure S2A. (C) Statistical analysis of currents elicited by application of PS (at concentrations indicated; blue bars), Nif (20 μM; red bars) and a combination of both substances (turquoise bars). Please note the different scale of the Y axes. The bars with two colours indicate the numerical sum of the currents obtained during application of PS and Nif alone. Inward currents (at −80 mV) at different concentrations of PS were evaluated separately. For quantitative analysis, all currents were normalized to the responses to 35 μM PS applied alone at the beginning and the end of each recording. Statistical tests were performed between the sum of the currents obtained during the separate application of a single substance (two-coloured bars) and the currents measured during co-application of both substances ($n = 7$–11).

caused a larger activation (i.e. larger currents) of TRPM3 than applying these substances alone (Figure 1B). Importantly, however, the currents observed when co-applying PS and nifedipine were also larger than the sum of the currents obtained with each substance alone (Figure 1B and C). We tested for supra-additivity over a wide range of concentrations (3.5 to 100 μM) of PS and found that even at the highest concentration of PS a robust supra-additive effect of nifedipine on the response to PS could be observed (Figure 1C). As argued in the Discussion, these data strongly favour a model in which PS and nifedipine act on TRPM3 channels via separate binding sites. Also, we observed that the supra-additive effect seemed larger at a holding potential of –80 mV compared with +80 mV (Figure 1C and data not shown). This indicates that addition of nifedipine changed the current–voltage relationship of the currents through TRPM3 channels by enhancing the inward currents more than the outward currents.

The effects of other 1,4-dihydropyridines on TRPM3 channel activity

Nifedipine is a labile compound that is easily degraded by radiation with visible light (Matsuda *et al.*, 1989). Hence, it is possible that the observed effects attributed to nifedipine are actually produced by one (or several) of its degradation products. We therefore tested whether photo-inactivated nifedipine still activates TRPM3 but found this not to be the case (Figure 2A). Hence, we assumed that nifedipine itself (which we carefully protected from light, especially when in solution) is responsible for the observed effects.

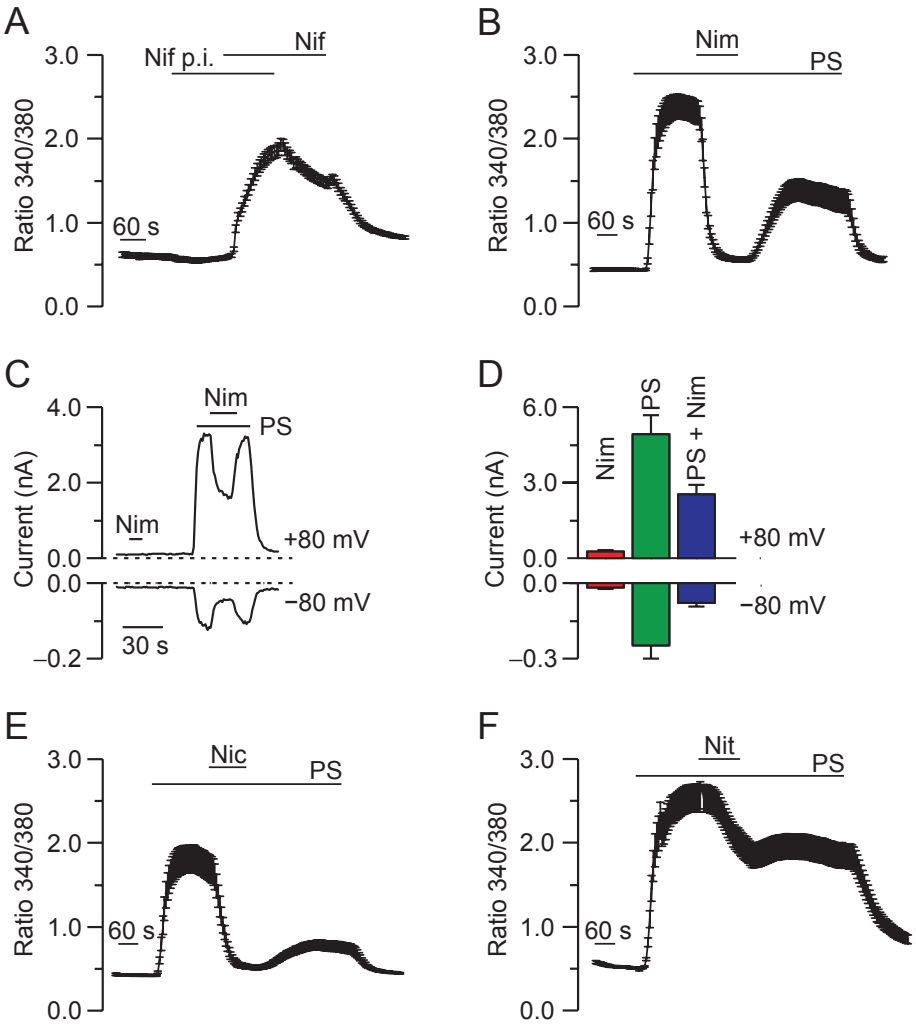

Figure 2

Effects of a variety of 1,4-dihydropyridines on TRPM3 channels. (A) During a Ca^{2+}-imaging experiment TRPM3-expressing cells were stimulated with 50 μM photo-inactivated nifedipine (Nif p.i.) and 50 μM not inactivated Nif as indicated (n = 56). (B) Similar experiment, using PS and nimodipine (both at 50 μM, n = 20). (C) Whole-cell patch-clamp measurement of a TRPM3-expressing cell obtained during similar experimental conditions as in (B), but using 21 μM PS and 21 μM nimodipine. The current–voltage relationships of this recording are given in Supporting Information Figure S2B. (D) Statistical analysis (n = 7) of currents measured in experiments performed as shown in (C). (E,F) Similar Ca^{2+}-imaging experiments as in (B), but using nicardipine (Nic) in (E) and nitrendipine (Nit) in (F) at 50 μM (n = 20 for each of the two panels).

We next co-applied a different 1,4-dihydropyridine, nimodipine (for structures of dihydropyridines see Supporting Information Table S1), together with PS. To our surprise, we found that nimodipine inhibited the PS-induced intracellular Ca^{2+} increase in TRPM3-expressing cells (Figure 2B). Accordingly, adding nimodipine to a PS-containing solution in whole-cell patch-clamp experiments caused a rapid and reversible decrease in current amplitude at all voltages (Figure 2C and D). Interestingly, adding nimodipine changed the shape of the current–voltage relationship, as inhibition at positive voltages (47.6 ± 1.6%, when applying nimodipine and nifedipine at a concentration of 21 μM) was significantly smaller than inhibition at negative voltages (70.2 ± 1.2%; $n = 7$; $P < 0.001$; Figure 2C and D). We next tried two other dihydropyridines and found that nicardipine also inhibited PS-induced TRPM3 activation (Figure 2E) while nitrendipine only had a small effect (Figure 2F). Similar results were obtained when activating TRPM3 with nifedipine (instead of PS; data not shown). These findings differentiate TRPM3 channels from TRPA1 channels, which are strongly activated by nifedipine, and also by nitrendipine, nimodipine and nicardipine (Fajardo *et al.*, 2008b). Collectively, these data show that 1,4-dihydropyridines have complex pharmacological actions on TRPM3 channels quite different from those on TRPA1 channels. Assuming that all dihydropyridines act on the same binding site when influencing TRPM3 channel activity, this binding site appears to be able to allosterically enhance or inhibit PS-activated TRPM3 channels, depending on the particular dihydropyridine compound binding to it.

The binding site of PS for TRPM3 activation is proteinaceous

PS is known to quickly and reversibly insert into the extracellular side of the plasma membrane thereby substantially increasing the electrical capacitance of the plasma membrane (Mennerick *et al.*, 2008). This insertion into the plasma membrane might also alter other biophysical properties of this lipid bilayer, such as fluidity or mechanical tension, some of which might cause the activation of TRPM3 channels. Alternatively, PS might activate TRPM3 channels by direct binding to a classical binding site. To distinguish between these two possibilities, we employed *ent*-PS, the synthetic enantiomer of PS (Nilsson *et al.*, 1998), which has identical biophysical properties to *nat*-PS, the naturally occurring enantiomer; specifically, the two enantiomers of PS induce the same change of membrane capacitance (Mennerick *et al.*, 2008). Using Ca^{2+}-imaging and whole-cell patch-clamp experiments, we found that *ent*-PS was substantially less capable of activating TRPM3 channels than *nat*-PS (Figure 3A–C). The quantitative analysis of the whole-cell patch-clamp data showed that the dose-response curve for *ent*-PS was shifted at least by a factor of 10 compared with the dose-response curve of *nat*-PS (Figure 3D). We also evaluated the change in membrane capacitance induced by applying *ent*-PS and *nat*-PS. In close agreement with the findings of Mennerick *et al.* (2008), we found only a marginal difference between *ent*-PS and *nat*-PS (Figure 3E) that cannot explain the large difference in TRPM3 activation found between *ent*-PS and *nat*-PS. Hence, we concluded that PS activates TRPM3 channels not by a non-specific membrane effect, but by binding to a specific proteinaceous binding site that is chirally selective.

Steroids inhibit the proton-activated outwardly rectifying anion current (PAORAC)

We and others previously reported that HEK293 cells endogenously express PAORACs that display a very steep outwardly rectifying current–voltage relationship (Nobles *et al.*, 2004; Lambert and Oberwinkler, 2005). Here, we report that these channels are inhibited by the extracellular application of PS (Figure 4). After activating these channels with an extracellular solution at pH 4, we found that the outward as well as the small inward currents were completely inhibited by applying 50 μM PS. This effect of PS was rapid and reversible (Figure 4A). Since this novel non-genomic effect of PS has not been described previously, we characterized it in more detail. We first investigated whether other steroids also had an inhibitory effect on PAORAC. While DHEA sulphate at 50 μM had a sizeable (but reduced, compared with PS) effect, pregnenolone, DHEA and progesterone (all at 50 μM) only slightly affected the PAORAC (Figure 4B and C). We then measured the dose-response curve for the inhibition of PAORAC by PS and DHEA sulphate (Figure 4C). Fitting the inhibition of the outward currents with Hill functions, we obtained IC_{50} values of 5.1 ± 1.6 μM for PS and 25.7 ± 1.1 μM for DHEA sulphate. These data show that PAORAC is inhibited by PS and, less potently, by DHEA sulphate. It is already recognized that these steroids can act as modulators of a variety of ion channels (Covey, 2009). However, our findings indicate that their rapid action on membrane proteins might even be more widespread than previously appreciated.

Inhibition of PAORAC by PS is not enantiomer-selective

Because we showed that the activation of TRPM3 by PS is much stronger for the naturally occurring enantiomer than for its synthetic enantiomer, we investigated whether this is also true for the inhibitory action of PS on PAORAC. We found this not to be the case. *ent*-PS and *nat*-PS both inhibited PAORAC completely at 50 μM (Figure 5A and B). At 5 μM the inhibition was only partial, but still to the same extent with both enantiomers (Figure 5D and E). Again, we obtained a control for the application of these steroids by evaluating the change in membrane capacitance induced by 50 μM PS and found no significant difference between *nat*-PS and *ent*-PS (Figure 5C). These data show that PS exhibited no enantiomer selectivity when inhibiting PAORAC. In the context of our study of TRPM3 channels, these data provide an important control because they reinforce the notion that some pharmacological effects of PS are not enantiomer-selective.

Structural requirements for steroidal TRPM3 agonists

Having established the existence of a chiral binding site for PS activation of TRPM3, we sought to identify further structural requirements for steroids to activate TRPM3. Firstly, we found that the double bond of PS (between position C5 and C6, see Supporting Information Table S2 for the numbering of

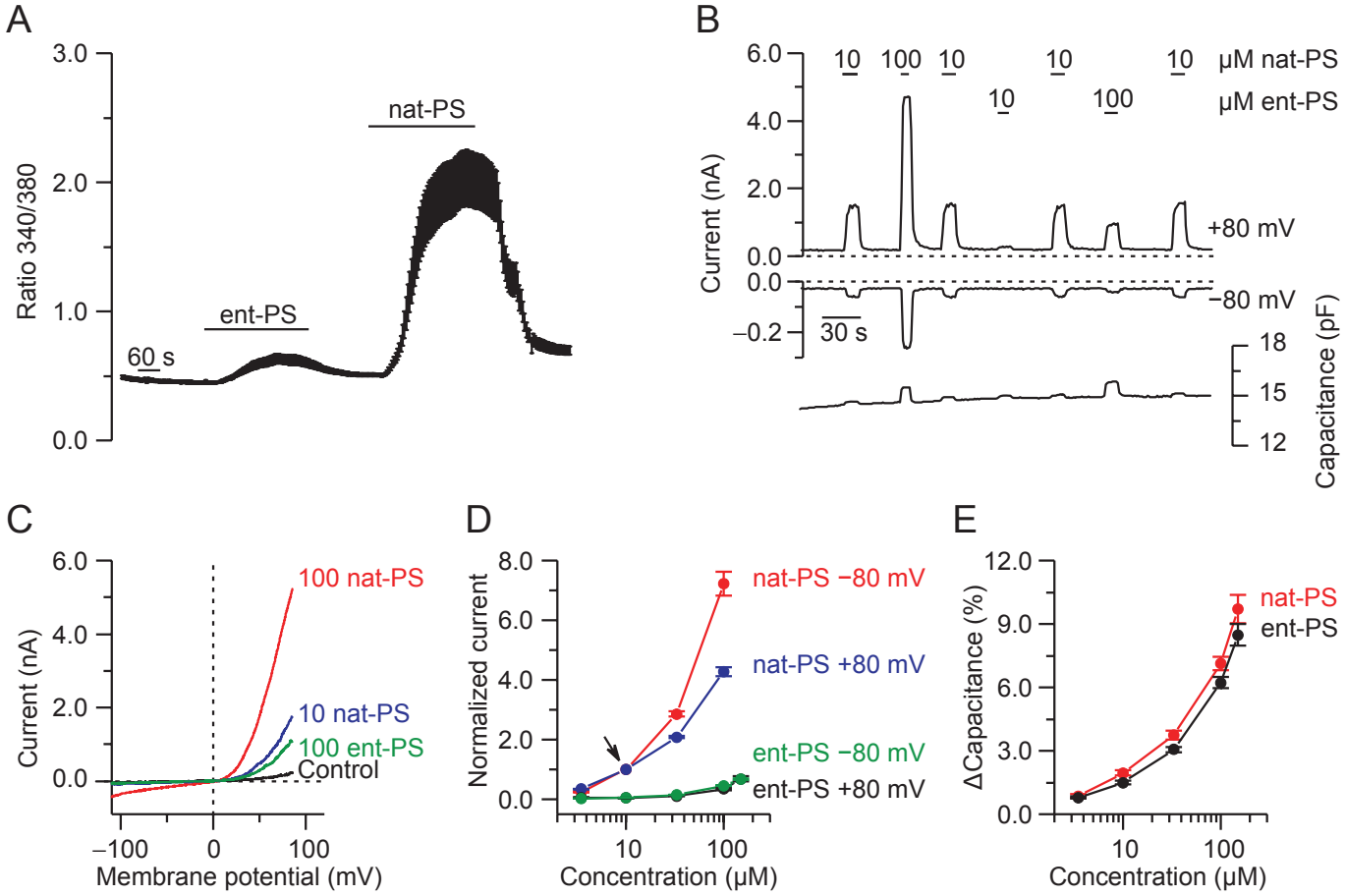

Figure 3

The two enantiomers of PS affect TRPM3 channels differentially. (A) TRPM3-expressing cells were superfused with *ent*-PS and *nat*-PS (both at 50 μM) in a Ca^{2+}-imaging experiment ($n = 19$). (B) Representative whole-cell patch-clamp recording from a TRPM3-expressing cell stimulated with *ent*-PS and *nat*-PS at the indicated concentrations. Upper panels show the current amplitude at +80 and −80 mV, lower panel depicts the apparent electrical capacitance. (C) Current–voltage relationships from the cell shown in (B). (D) Statistical analysis of cells (n = 12–38 per data point) recorded in similar experiments to those shown in (B). Inward and outward currents were normalized separately to the current amplitude measured with 10 μM *nat*-PS (arrow). (E) Dose-response curve for capacitance increase found for *ent*-PS and *nat*-PS during experiments conducted similarly to those shown in (B).

steroid C atoms) was not strictly required for the activation of TRPM3, as 50 μM epipregnanolone sulphate (3β,5β-pregnanolone sulphate) also activated TRPM3, albeit to a much lesser degree than PS (Figure 6A). The β-orientation of the sulphate group at the C3 position, however, proved to be important, as the compound with the corresponding α-orientation (3α,5β-pregnanolone sulphate or pregnanolone sulphate) was entirely ineffective at activating TRPM3 channels (Figure 6C). These data are qualitatively similar to those reported by Majeed *et al.* (2010) but show quantitative differences. More importantly, however, epiallopregnanolone sulphate (3β,5α-pregnanolone sulphate) induced an increase in intracellular Ca^{2+} comparable to PS, and much larger than that induced by its epimer epipregnanolone sulphate (3β,5β-pregnanolone sulphate; Figure 6B and C). In order to quantify these effects more precisely, we turned again to patch-clamp electrophysiology and obtained dose-response curves for the activation of TRPM3 channels by epipregnanolone sulphate and epiallopregnanolone sulphate (Figure 6D and E). The results confirm that epiallopregnanolone sulphate activated TRPM3 with a very similar potency to that of PS, while the potency of epipregnanolone sulphate was approximately 10-fold less. Previously, we reported that pregnenolone was a much weaker agonist for TRPM3 channels compared with PS (Wagner *et al.*, 2008), indicating that the sulphate group in position C3 is important. We added additional weight to this conclusion by using epiallopregnanolone. In contrast to epiallopregnanolone sulphate, this compound had only marginal effects on TRPM3 channels (Figure 6C). Together, these data indicate that the double bond between C5 and C6 of PS is not required and that 5α-reduced steroids can strongly activate TRPM3 channels. In contrast, 5β-reduced steroids only activated TRPM3 channels weakly or not at all. These data also suggest that the presence of the sulphate group is important for TRPM3 activation, as is its stereochemical orientation. For the compounds investigated here, the required orientation for the sulphate group at the C3 position was 3β.

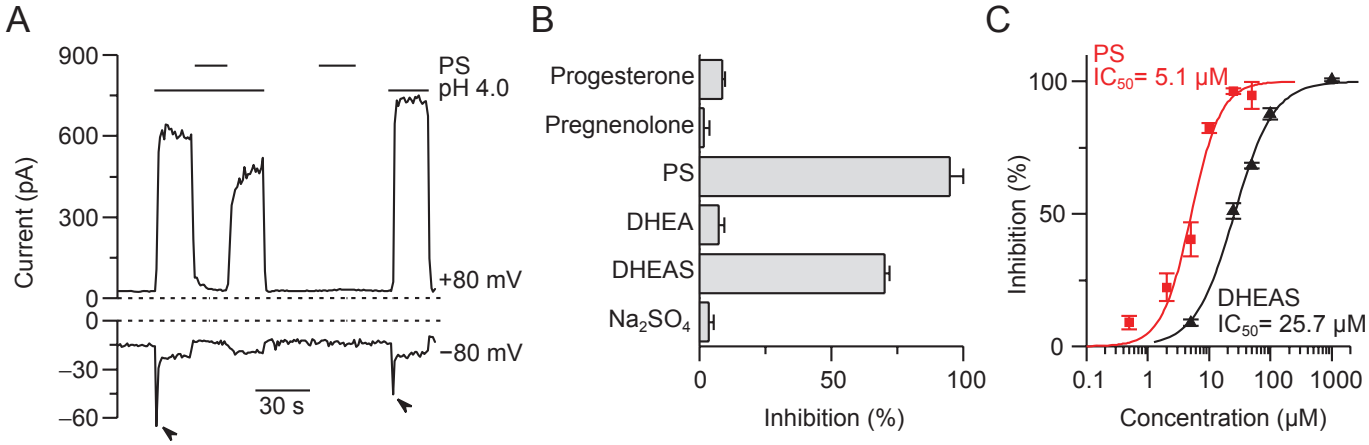

Figure 4

PAORAC are inhibited by PS and dehydroepiandrosterone (DHEA) sulphate. (A) Current traces of HEK293 cells at membrane potentials of –80 and +80 mV during application of acidic solution (pH 4) and PS. Arrowheads designate quickly inactivating currents presumably caused by the activation of acid-sensing ion channels known to be expressed in HEK293 cells (Gunthorpe *et al.*, 2001). These currents were not further investigated. Current–voltage relationships obtained in this recording were typical for PAORAC currents and are displayed in Supporting Information Figure S2C. (B) Statistical analysis of the inhibition of the pH 4-evoked current induced by the indicated substances at a concentration of 50 μM (n = 5–6, for each substance). Outward currents (at +80 mV) were analysed from experiments performed as shown in (A). (C) Normalized dose-response curves established from experiments comparable to those shown in (A) at a membrane potential of +80 mV. The continuous lines were obtained by fits to the Hill function, which yielded an IC_{50} = 5.1 ± 1.1 μM and a Hill coefficient = 1.8 ± 0.4 for PS and an IC_{50} = 25.7 ± 1.1 μM and a Hill coefficient = 1.4 ± 0.1 for DHEA sulphate (n = 5–8, for each data point).

Effects of other negatively charged substituents at the C3 position

To further pinpoint the structural requirements of the substituent at the C3 position, we performed a series of experiments in which the sulphate group was exchanged for other groups. We found that replacing the sulphate group with an uncharged group (pregnenolone methyl ether and pregnenolone acetate) completely or almost completely abolished activation of TRPM3 channels, as judged by Ca^{2+}-imaging experiments (Figure 7A). The data on pregnenolone acetate are in excellent agreement with recently published data on human TRPM3 channels (Majeed *et al.*, 2010). Furthermore we could not detect any activation of TRPM3 by 3β-acetates in electrophysiological experiments, irrespective of whether the hydrogen at the C5 was in the α- or β-orientation (Figure 7B and C). However, when the C3 sulphate group was replaced with glucuronidate or hemisuccinate, the resulting compounds retained some (pregnenolone glucuronidate) or a substantial part (pregnenolone hemisuccinate) of their capacity to activate TRPM3 channels (Figure 7A). Interestingly, both the glucuronidate and hemisuccinate groups carry a carboxylate moiety, which should be negatively charged at the physiological pH values used in these experiments. These data therefore support the notion that a negative charge for the group at the C3 position in β-orientation is of great importance for activating TRPM3 channels.

Discussion

The experiments presented in this manuscript allow us to draw three major conclusions: firstly, the dihydropyridine nifedipine and the steroid PS bind to separate binding sites for activating TRPM3 channels. Secondly, the steroid PS binds to an enantiomer-selective, and thus proteinaceous binding site. Finally, key structural features of the binding site for PS are determined.

Nifedipine and PS bind to separate binding sites

Co-application of nifedipine and PS induced responses of TRPM3 channels that were larger than the sum of the individual responses to the single compounds, demonstrating supra-additivity. Nevertheless, this observed supra-additivity does not necessarily mean that the two substances act on different binding sites because supra-additive behaviour can, in principle, also occur if the substances bind to the same binding site, provided that the dose-response curve is steep (Hill coefficient larger than one). This might be relevant for TRPM3 because we reported Hill coefficients of 1.7 to 1.9 for the dose-response curves of TRPM3 channels activated by PS and nifedipine (Wagner *et al.*, 2008). However, supra-additivity solely due to a steep dose-response curve only occurs at low agonist concentrations, because even for very high Hill coefficients the slope of the dose-response curves levels off at higher concentrations. It can be shown that for concentrations larger than 1.33 times the EC_{50} value, all Hill functions (even those with very large Hill coefficients) display sub-linear (i.e. less than additive) behaviour. Importantly, we observed supra-additive behaviour at PS concentrations up to 100 μM (Figure 1C), which is more than four times larger than our estimate of the EC_{50} value (23 μM; Wagner *et al.*, 2008). These considerations strongly suggest that the observed supra-additive behaviour is not only due to the steep dose-response curve. Therefore, the supra-additivity

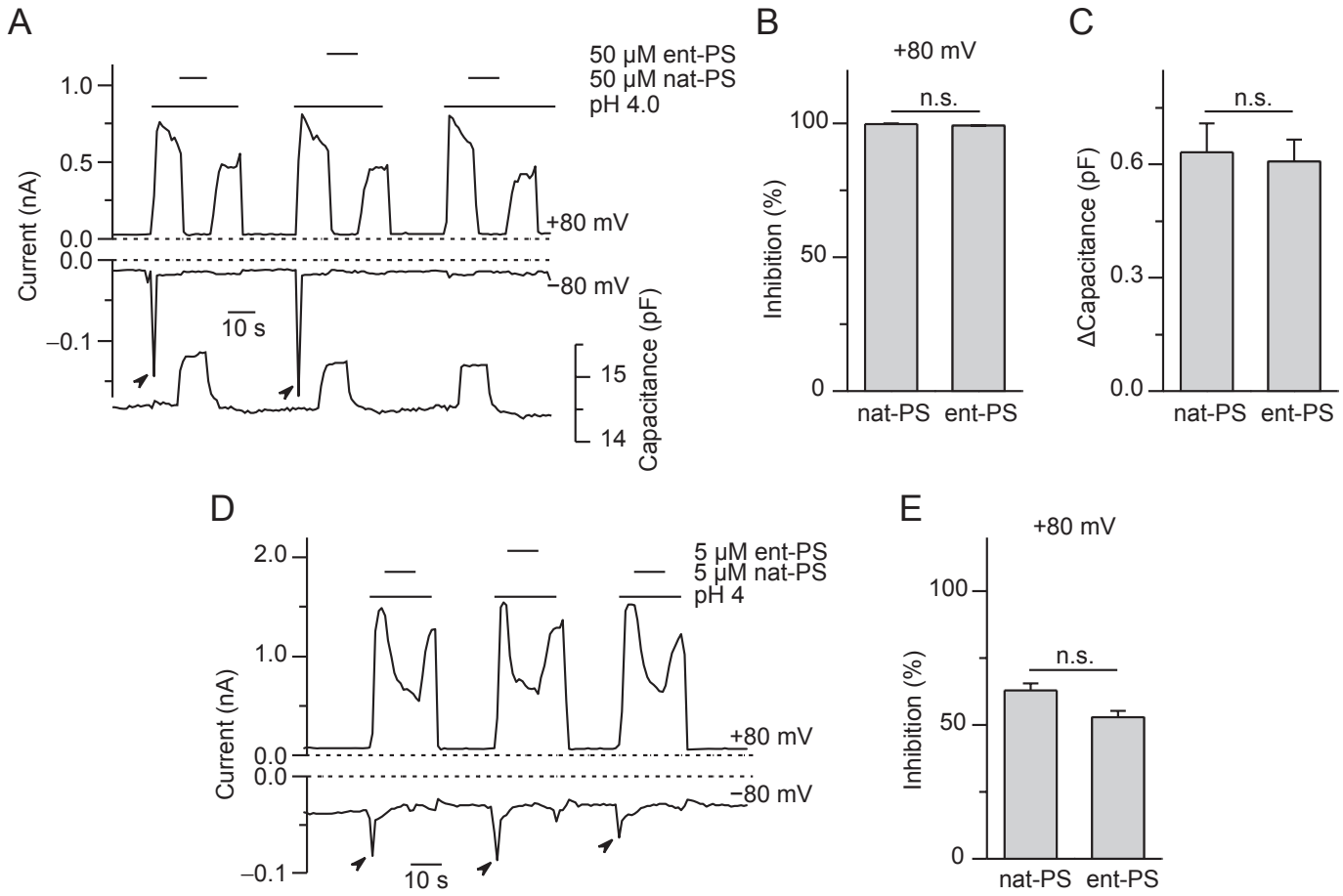

Figure 5

Both enantiomers of PS inhibit PAORAC with similar potency. (A) Current traces obtained from a HEK293 cell at membrane potentials of −80 and +80 mV. The lower panel shows a capacitance trace of this recording. The application of acidic solution (pH 4) and *nat*-PS or *ent*-PS (both at 50 μM) is indicated. (B) Statistical analysis ($n = 7$) of the inhibition of the pH 4-evoked current at +80 mV. (C) Statistical comparison ($n = 7$) of membrane capacitance changes during application of *nat*-PS or *ent*-PS. (D) Similar experiment as in (A) but employing a lower concentration (5 μM) of steroids. (E) Statistical analysis ($n = 5$) of the experiments performed as shown in (D). Arrowheads in (A) and (D) indicate Acid-sensing ion channel-like inward currents at the beginning of exposure to acidic solutions. Current–voltage relationships of the recordings shown in panel (A) and (D) are depicted in Supporting Information Figure S2D and E.

cannot be explained by the presence of only one type of binding site and we conclude that the two substances bind to two different, but positively interacting binding sites.

Previously, we reported that other dihydropyridines, such as nicardipine and nimodipine, do not activate TRPM3 channels (Wagner *et al.*, 2008). Here, we demonstrated that these substances actually inhibit TRPM3. Structurally, the dihydropyridines showing a strong inhibition of TRPM3 channels (nicardipine and nimodipine, Figure 2) have bulkier side groups on at least one side (compared with the methyl ester of nifedipine, Supporting Information Table S1), which might explain their inhibitory action. Alternatively, the position of the nitro-group on the phenyl ring, which differs between nifedipine and the other dihydropyridines, might also play a role.

PS binds to a proteinaceous binding site

PS inserts reversibly into the plasma membrane and alters its biophysical properties. This has been directly demonstrated by measuring the increase in electrical capacitance of the plasma membrane during application of PS (Mennerick *et al.*, 2008). Therefore, it is conceivable that TRPM3 is activated by PS indirectly through a change in biophysical membrane properties. Alternatively, PS might act by binding to a binding site of a protein. One way to solve this question is the use of enantiomeric substances, as enantiomers have the exact same physical properties, but are likely to bind with different affinities to proteinaceous and thus chiral binding sites. Our data using enantiomers of PS clearly demonstrate that the unnatural enantiomer of PS is dramatically less potent than the natural one, strongly indicating that PS needs to bind to a chiral and thus proteinaceous binding site. Previously, Majeed *et al.* (2010) reported similar experiments performed with diastereomers of pregnanolone sulphate (epipregnanolone sulphate and pregnanolone sulphate) and androsterone sulphate (androsterone sulphate and epiandrosterone sulphate). However, pairs of diastereomers do not have the same physical properties and

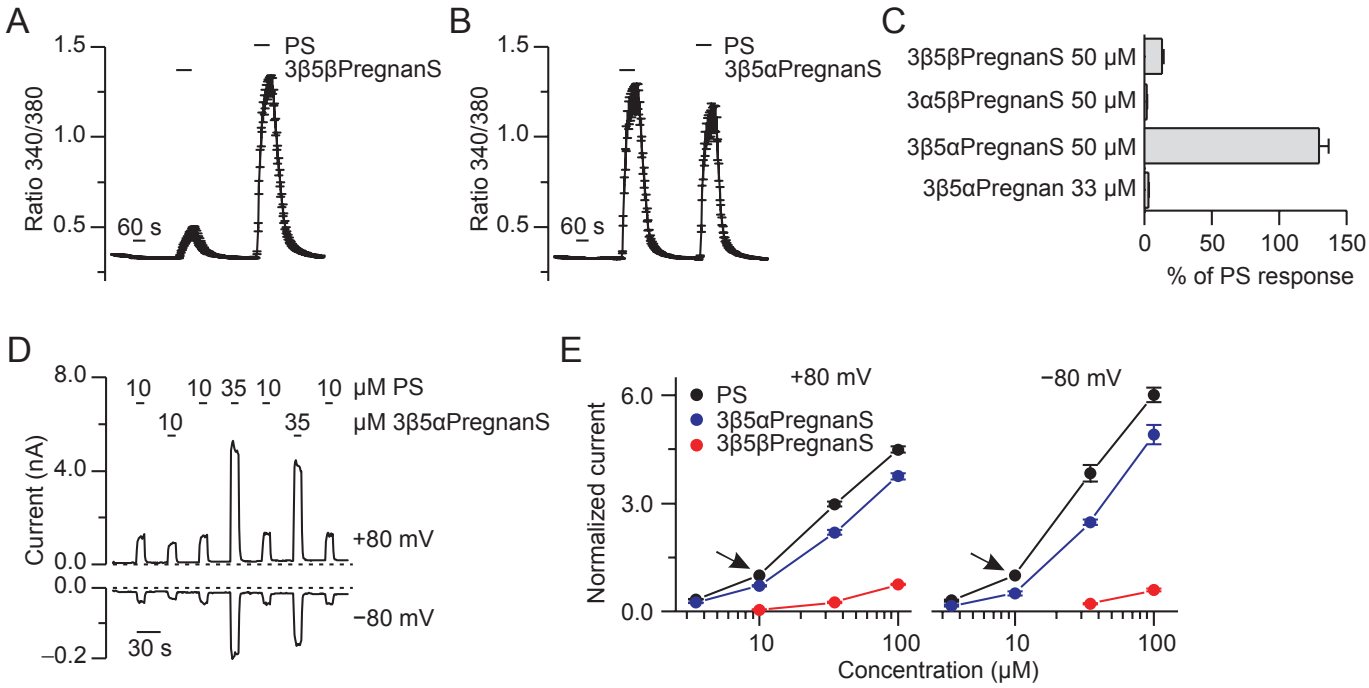

Figure 6

The effects of the configuration at the C3 and C5 positions on the activity of TRPM3 channels. (A) Changes in intracellular calcium measured in TRPM3-transfected cells are shown during the application of PS and epipregnanolone sulphate (3β5βPregnanS), both at 50 μM (n = 55). (B) Similar experiment with 50 μM epiallopregnanolone sulphate (3β5αPregnanS), which evokes a similar response to that of PS (n = 36). (C) Summary of stimulatory effects of the indicated substances on TRPM3 channels. Increases in the 340/380 ratio were evaluated, averaged (n = 20–55) and normalized to the response to PS (same concentration as test compound) of the same cell. Untransfected HEK293 cells did not respond to these substances (not shown). (D) Electrophysiological recording of a TRPM3-expressing cell (at +80 and −80 mV) stimulated with PS or epiallopregnanolone sulphate (3β5αPregnanS) at the indicated concentration. The current–voltage relationships of this recording are shown in Supporting Information Figure S2F. (E) Dose-response curves obtained from experiments (n = 8–11) similar to those shown in (D). Amplitudes of outward currents (+80 mV, left panel) and of inward currents (−80 mV, right panel) were independently normalized to the response to 10 μM PS (arrows).

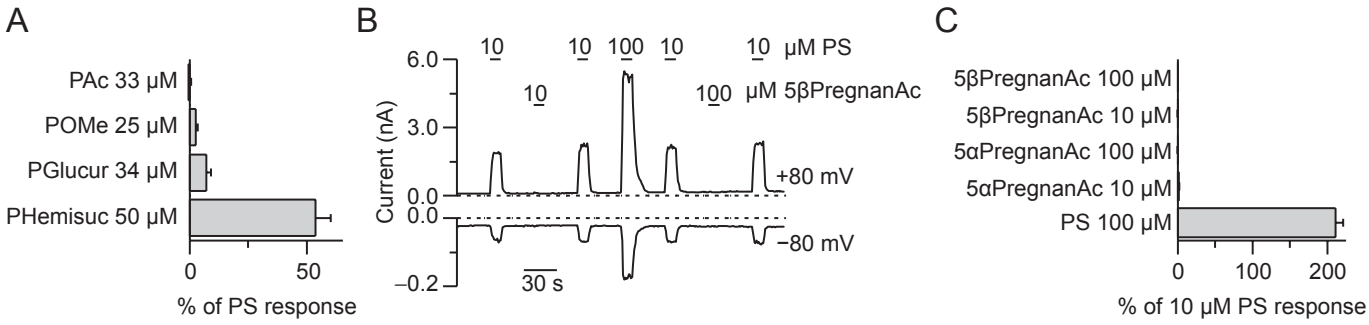

Figure 7

A negative charge at the C3 position of steroids is necessary to activate TRPM3 channels. (A) Summary of Ca^{2+}-imaging experiments on TRPM3-expressing cells with PS-analogues in which the sulphate group had been substituted either with acetate (PAc), methyl ether (POMe), glucuronic acid (PGlucur) or hemisuccinate (PHemisuc). Increases in fluorescence ratio values were normalized to the response to PS at the same concentration as the test substance (n = 20–43). Pregnenolone hemisuccinate also induced a small signal in untransfected HEK293 cells indicating a minor TRPM3-independent effect (data not shown). (B) Electrophysiological recording of a TRPM3-expressing cell stimulated with 3β,5β-pregnanolone-acetate (3β5βPregnanAc) or PS at the indicated concentration. Current–voltage relationships from this recording are plotted in Supporting Information Figure S2G. (C) Summary of electrophysiological experiments (n = 6) showing that neither 3β,5α-pregnanolone acetate (5αPregnanAc) nor 3β,5β-pregnanolone acetate was capable of stimulating TRPM3 channels, even at high concentrations (100 μM).

therefore are not suited to answer the question outlined above decisively.

We used several controls to validate our data: firstly, we concomitantly measured the currents through TRPM3 channels and monitored the membrane capacitance, as this parameter increases upon application of PS (Mennerick *et al*., 2008) independently of TRPM3 channels. The measurements of the membrane capacitance thus allowed us to control for whether we were applying equal amounts of both enantiomers (Figures 3E and 5C). Also, we exploited the serendipitous discovery that PAORAC currents (Lambert and Oberwinkler, 2005) are inhibited by PS. For PAORAC, we found that the effects of both PS enantiomers were comparable. We thus concluded that PAORAC can be inhibited by PS without PS necessarily binding to a enantio-specific binding site. The published findings of enantiomeric selectivity of effects exerted by PS on other ion channels (reviewed by Covey, 2009) fit well with our conclusions. $GABA_A$ and NMDA receptors from rats are inhibited by PS in a non-enantioselective fashion (Nilsson *et al*., 1998; Vallée *et al*., 2001), similar to our findings with PAORAC. In contrast, the UNC-49 GABA receptor of *Caenorhabditis elegans* shows enantiomeric selectivity when being inhibited by PS (Twede *et al*., 2007). However, the difference in IC_{50} values between the two PS enantiomers was only threefold for UNC-49. This contrasts strongly with the impressive (>10-fold) enantioselective effect that we observed for TRPM3 (Figure 3), which is, therefore, the ion channel with the strongest enantioselectivity for PS known to date. Possibly, the strong enantioselective effect that we found for TRPM3 is still an underestimate of the true magnitude of the effect because the *ent*-PS sample contains 1.4% *nat*-PS, which thus might have caused part of the residual response to *ent*-PS.

Together, our data establish that TRPM3 is activated when PS binds to a specific binding site on a protein. This finding fits very well to the biochemical data obtained by Majeed *et al*. (2012) showing that binding of TRPM3-containing membranes to PS is increased compared with membranes not containing TRPM3. It is, however, important to note that none of the available data allows one to conclude unequivocally that the specific binding site of PS is on the TRPM3 proteins themselves. Rather, the possibility that TRPM3 assembles with an – as yet unknown – other protein, which provides the PS binding site, in a quaternary complex needs to be considered. As activation of TRPM3 channels by PS has been shown to work in a variety of cell types, such an auxiliary protein would need to be expressed ubiquitously. Additionally, the interaction between such a hypothetical auxiliary protein and TRPM3 proteins would need to be strong in order to resist the depletion of the plasma membrane of cholesterol. Such a treatment (achieved by incubating the cells with methyl-β-cyclodextrin) has been shown to enhance rather than to diminish the PS-induced activity of TRPM3 channels (Naylor *et al*., 2010). We repeated these experiments (Supporting Information Figure S3) and confirmed that methyl-β-cyclodextrin treatment also increases the PS-induced activity of mouse TRPM3 channels, while additional cholesterol (administered as a methyl-β-cyclodextrin/cholesterol complex) reduces mouse TRPM3 channel activity, as demonstrated previously for human TRPM3 channels (Naylor *et al*., 2010).

Potency of structural analogues of PS at activating TRPM3 channels

It was shown that removal of the sulphate group at the C3 position (yielding pregnenolone) strongly reduced the efficacy of PS (Wagner *et al*., 2008), while replacing the sulphate with acetate completely abolished the activity of this compound (Majeed *et al*., 2010). Furthermore, Majeed *et al*. (2010) found that the sulphate group needs to be in the β-configuration, as epipregnanolone sulphate (3β) more strongly activated TRPM3 channels than pregnanolone sulphate (3α). Equally, epiandrosterone sulphate (3β) was much more efficient than androsterone sulphate (3α).

We expanded this knowledge by showing that pregnenolone acetate, as well as 3β,5α-pregnanolone acetate and 3β,5β-pregnanolone acetate are not capable of activating murine TRPM3 channels, which is in excellent agreement with the findings on human TRPM3 channels (Majeed *et al*., 2010). Similarly, we found that pregnenolone methyl ether did not activate TRPM3 channels. We employed further compounds in which the sulphate in the C3 position was replaced with a group retaining some negative charge. Interestingly, these compounds – pregnenolone glucuronidate and pregnenolone hemisuccinate – were both considerably effective at activating TRPM3 channels (Figure 7). We interpret these findings as providing strong support that in order for the steroids to be effective at activating TRPM3, a negative charge is needed at their C3 position.

Finally, we found that epiallopregnanolone sulphate (3β,5α-pregnanolone sulphate) activates TRPM3 channels almost as strongly as PS. This is in contrast to pregnanolone sulphate (3α,5β-pregnanolone sulphate) and epipregnanolone sulphate (3β,5β-pregnanolone sulphate), which were either entirely ineffective or weak activators of TRPM3 channels, respectively (Figure 6). These data can be compared with those published by Majeed *et al*. (2010) who also used pregnanolone sulphate and epipregnanolone sulphate. For epipregnanolone sulphate, Majeed *et al*. (2010) found that it activated human TRPM3 channels more strongly than we found for murine TRPM3 channels. The origin of the observed differences is unclear but may be due to the species difference. Overall, however, these observed quantitative differences appear to be minor given the impressive similarity in the pharmacological profile of human and murine TRPM3 channels (Wagner *et al*., 2008; Majeed *et al*., 2010).

In order to rationalize our findings, we aligned the chemical structure of the compounds tested and found – in considerable agreement with our experimental findings – that epiallopregnanolone sulphate can be very well aligned to PS with only very minor structural deviations (Supporting Information Figure S4A). Epipregnanolone sulphate (Supporting Information Figure S4B), and even more so pregnanolone sulphate (Supporting Information Figure S4C), showed more pronounced differences in their alignment with PS, especially with respect to the A-ring and substituents bound to it. These findings help to visualize and to appreciate why epiallopregnanolone sulphate activates TRPM3 almost as strongly as PS, in contrast to its diastereomers.

Properties of the PS binding site

Together with information from the literature, our results can be used to deduce some properties of the binding site for

steroids. Because the negative charge at the C3 position is very important for activating TRPM3, we conclude that it probably interacts with a positively charged residue on the interacting protein. Furthermore, the finding that 5β-reduced steroids (pregnanolone sulphate and epipregnanolone sulphate) were considerably less effective at activating TRPM3 channels than 5α-reduced steroids suggests a flat and elongated binding pocket (Supporting Information Figure S4A–C), or that the steroids must pass a channel of such a shape for accessing the binding site. This might also be one of the reasons why steroids with a 3α-configuration activated TRPM3 channels less strongly then their 3β-diastereomers.

It is interesting to ask why *ent*-PS is such a poor substitute for *nat*-PS. Assuming that *ent*-PS binds to the same binding site and in the same orientation as *nat*-PS (Supporting Information Figure S4D), two features of *ent*-PS might reduce its effectiveness: the aforementioned orientation of the sulphate at the C3 position (3α) and the methyl groups at C18 and C19 that protrude from the flat steroid in the opposite direction. However, it has been shown that *ent*-steroids can also bind to ion channels in a flipped (rotated by 180°, Supporting Information Figure S4E) orientation (Krishnan *et al*., 2012). In this orientation, neither the group at C3 (which has now exactly the same orientation as for *nat*-PS) nor the C18/C19 methyl groups (which now project to the same side) can hinder the binding (or the access) of *ent*-PS. Instead, in this orientation, the B and D rings of the backbone and/or the carbon side chain at C17 differ substantially between the superimposed *ent*-PS and *nat*-PS. Since *ent*-PS is such a poor replacement for *nat*-PS in activating TRPM3, *ent*-PS does not seem to bind well in either of these two orientations. This in turn suggests that the binding site (or the access to it) is rather tight and well matched to the shape of *nat*-PS. This then explains the remarkably narrow structure–activity relationship observed experimentally.

PS inhibits PAORAC

While investigating the effects of steroids on TRPM3, we serendipitously discovered that PS also inhibits the endogenous PAORACs in HEK293 cells (Nobles *et al*., 2004; Lambert and Oberwinkler, 2005). Recently, it was hypothesized that these channels are encoded by ClC-3 proteins, which belong to the group of ClC proteins most of which were first described as anion channels but are now recognized as Cl^-/H^+ antiporters (Zifarelli and Pusch, 2007; Stauber *et al*., 2012). It was proposed that ClC-3 displays an uncoupled mode of anion transfer in strongly acidic extracellular conditions (Matsuda *et al*., 2008; 2010; Wang *et al*., 2012). However, this view has recently been challenged (Guzman *et al*., 2013; Sato-Numata *et al*., 2013), and the molecular identity of PAORAC is, therefore, still an open question. The dearth of selective pharmacological tools to study these channels has arguably been a cause for the lack of deeper understanding of these channels. PS and its interesting mode of action (possibly through non-specific effects on the biophysical properties of the membrane) might therefore offer new clues and possibilities to study these mysterious channels.

Summary

In this study, we have provided strong evidence that the steroid PS and the dihydropyridine nifedipine activate TRPM3 channels through different binding sites. We formally proved that the binding site for PS is chiral and thus proteinaceous in nature and have increased the understanding of the structural requirements imposed on steroids for effective activation of TRPM3 channels. Our data will guide future efforts to design improved agonists and antagonists of these channels and reinforce the emerging concept that steroid binding to TRPM3 channels has a narrow structure–activity relationship.

Acknowledgements

We thank Sandra Plant, Melanie Portz and Raissa Wehmeyer for excellent technical support. This study was funded by the DFG (Emmy Noether-programme, GK 1326 and SFB 593) and by the NIH grant GM47969 (to D F C). We thank Drs M X Zhu and C Halaszovich for helpful discussions and Franziska Schneider and Christian Goecke for critically reading the manuscript.

Conflict of interest

None.

References

Abràmoff MD, Magalhães PJ, Ram SJ (2004). Image processing with ImageJ. Biophotonics Int 11: 36–42.

Alexander SPH, Benson HE, Faccenda E, Pawson AJ, Sharman JL, Catterall WA, Spedding M, Peters JA, Harmar AJ and CGTP Collaborators (2013). The Concise Guide to PHARMACOLOGY 2013/14: Overview. Br J Pharmacol 170: 1449–1867.

Bagal SK, Brown AD, Cox PJ, Omoto K, Owen RM, Pryde DC *et al*. (2013). Ion channels as therapeutic targets: a drug discovery perspective. J Med Chem 56: 593–624.

Behrendt M, Keiser M, Hoch M, Naim HY (2009). Impaired trafficking and subcellular localization of a mutant lactase associated with congenital lactase deficiency. Gastroenterology 136: 2295–2303.

Covey DF (2009). ent-Steroids: novel tools for studies of signaling pathways. Steroids 74: 577–585.

Düfer M, Hörth K, Wagner R, Schittenhelm B, Prowald S, Wagner TFJ *et al*. (2012). Bile acids acutely stimulate insulin secretion of mouse β-cells via farnesoid X receptor activation and K(ATP) channel inhibition. Diabetes 61: 1479–1489.

Fajardo O, Meseguer V, Belmonte C, Viana F (2008a). TRPA1 channels mediate cold temperature sensing in mammalian vagal sensory neurons: pharmacological and genetic evidence. J Neurosci 28: 7863–7875.

Fajardo O, Meseguer V, Belmonte C, Viana F (2008b). TRPA1 channels: novel targets of 1,4-dihydropyridines. Channels (Austin) 2: 429–438.

Fonfria E, Murdock PR, Cusdin FS, Benham CD, Kelsell RE, McNulty S (2006). Tissue distribution profiles of the human TRPM cation channel family. J Recept Signal Transduct Res 26: 159–178.

Frühwald J, Camacho Londoño J, Dembla S, Mannebach S, Lis A, Drews A *et al*. (2012). Alternative splicing of a protein domain indispensable for function of transient receptor potential melastatin 3 (TRPM3) ion channels. J Biol Chem 287: 36663–36672.

Grimm C, Kraft R, Sauerbruch S, Schultz G, Harteneck C (2003). Molecular and functional characterization of the melastatin-related cation channel TRPM3. J Biol Chem 278: 21493–21501.

Grimm C, Kraft R, Schultz G, Harteneck C (2005). Activation of the melastatin-related cation channel TRPM3 by D-erythro-sphingosine [corrected]. Mol Pharmacol 67: 798–805.

Gunthorpe MJ, Smith GD, Davis JB, Randall AD (2001). Characterisation of a human acid-sensing ion channel (hASIC1a) endogenously expressed in HEK293 cells. Pflugers Arch 442: 668–674.

Guzman RE, Grieschat M, Fahlke C, Alekov AK (2013). ClC-3 is an intracellular chloride/proton exchanger with large voltage-dependent nonlinear capacitance. ACS Chem Neurosci 4: 994–1003.

Klose C, Straub I, Riehle M, Ranta F, Krautwurst D, Ullrich S *et al*. (2011). Fenamates as TRP channel blockers: mefenamic acid selectively blocks TRPM3. Br J Pharmacol 162: 1757–1769.

Krishnan K, Manion BD, Taylor A, Bracamontes J, Steinbach JH, Reichert DE *et al*. (2012). Neurosteroid analogues. 17. Inverted binding orientations of androsterone enantiomers at the steroid potentiation site on γ-aminobutyric acid type A receptors. J Med Chem 55: 1334–1345.

Kunert-Keil C, Bisping F, Krüger J, Brinkmeier H (2006). Tissue-specific expression of TRP channel genes in the mouse and its variation in three different mouse strains. BMC Genomics 7: 159.

Lambert S, Oberwinkler J (2005). Characterization of a proton-activated, outwardly rectifying anion channel. J Physiol 567: 191–213.

Lambert S, Drews A, Rizun O, Wagner TFJ, Lis A, Mannebach S *et al*. (2011). Transient receptor potential melastatin 1 (TRPM1) is an ion-conducting plasma membrane channel inhibited by zinc ions. J Biol Chem 286: 12221–12233.

Lee N, Chen J, Sun L, Wu S, Gray KR, Rich A *et al*. (2003). Expression and characterization of human transient receptor potential melastatin 3 (hTRPM3). J Biol Chem 278: 20890–20897.

Majeed Y, Agarwal AK, Naylor J, Seymour VAL, Jiang S, Muraki K *et al*. (2010). Cis-isomerism and other chemical requirements of steroidal agonists and partial agonists acting at TRPM3 channels. Br J Pharmacol 161: 430–441.

Majeed Y, Tumova S, Green BL, Seymour VAL, Woods DM, Agarwal AK *et al*. (2012). Pregnenolone sulphate-independent inhibition of TRPM3 channels by progesterone. Cell Calcium 51: 1–11.

Matsuda JJ, Filali MS, Volk KA, Collins MM, Moreland JG, Lamb FS (2008). Overexpression of CLC-3 in HEK293T cells yields novel currents that are pH dependent. Am J Physiol Cell Physiol 294: C251–C262.

Matsuda JJ, Filali MS, Collins MM, Volk KA, Lamb FS (2010). The ClC-3 Cl^-/H^+ antiporter becomes uncoupled at low extracellular pH. J Biol Chem 285: 2569–2579.

Matsuda Y, Teraoka R, Sugimoto I (1989). Comparative evaluation of photostability of solid-state nifedipine under ordinary and intensive light irradiation conditions. Int J Pharm 54: 211–221.

Mennerick S, Lamberta M, Shu H-J, Hogins J, Wang C, Covey DF *et al*. (2008). Effects on membrane capacitance of steroids with antagonist properties at $GABA_A$ receptors. Biophys J 95: 176–185.

Moran MM, McAlexander MA, Bíró T, Szallasi A (2011). Transient receptor potential channels as therapeutic targets. Nat Rev Drug Discov 10: 601–620.

Naylor J, Li J, Milligan CJ, Zeng F, Sukumar P, Hou B *et al*. (2010). Pregnenolone sulphate- and cholesterol-regulated TRPM3 channels coupled to vascular smooth muscle secretion and contraction. Circ Res 106: 1507–1515.

Nilsson KR, Zorumski CF, Covey DF (1998). Neurosteroid analogues. 6. The synthesis and $GABA_A$ receptor pharmacology of enantiomers of dehydroepiandrosterone sulfate, pregnenolone sulfate, and (3α,5β)-3-hydroxypregnan-20-one sulfate. J Med Chem 41: 2604–2613.

Nobles M, Higgins CF, Sardini A (2004). Extracellular acidification elicits a chloride current that shares characteristics with $I_{Cl(swell)}$. Am J Physiol Cell Physiol 287: C1426–C1435.

Oberwinkler J, Philipp SE (2007). TRPM3. Handb Exp Pharmacol 179: 253–267.

Oberwinkler J, Lis A, Giehl KM, Flockerzi V, Philipp SE (2005). Alternative splicing switches the divalent cation selectivity of TRPM3 channels. J Biol Chem 280: 22540–22548.

Sato-Numata K, Numata T, Okada T, Okada Y (2013). Acid-sensitive outwardly rectifying (ASOR) anion channels in human epithelial cells are highly sensitive to temperature and independent of ClC-3. Pflugers Arch 465: 1535–1543.

Stauber T, Weinert S, Jentsch TJ (2012). Cell biology and physiology of CLC chloride channels and transporters. Compr Physiol 2: 1701–1744.

Straub I, Krügel U, Mohr F, Teichert J, Rizun O, Konrad M *et al*. (2013a). Flavanones that selectively inhibit TRPM3 attenuate thermal nociception in vivo. Mol Pharmacol 84: 736–750.

Straub I, Mohr F, Stab J, Konrad M, Philipp SE, Oberwinkler J *et al*. (2013b). Citrus fruit and fabacea secondary metabolites potently and selectively block TRPM3. Br J Pharmacol 168: 1835–1850.

Twede V, Tartaglia AL, Covey DF, Bamber BA (2007). The neurosteroids dehydroepiandrosterone sulfate and pregnenolone sulfate inhibit the UNC-49 GABA receptor through a common set of residues. Mol Pharmacol 72: 1322–1329.

Vallée M, Shen W, Heinrichs SC, Zorumski CF, Covey DF, Koob GF *et al*. (2001). Steroid structure and pharmacological properties determine the anti-amnesic effects of pregnenolone sulphate in the passive avoidance task in rats. Eur J Neurosci 14: 2003–2010.

Vriens J, Owsianik G, Hofmann T, Philipp SE, Stab J, Chen X *et al*. (2011). TRPM3 is a nociceptor channel involved in the detection of noxious heat. Neuron 70: 482–494.

Wagner TFJ, Loch S, Lambert S, Straub I, Mannebach S, Mathar I *et al*. (2008). Transient receptor potential M3 channels are ionotropic steroid receptors in pancreatic β cells. Nat Cell Biol 10: 1421–1430.

Wagner TFJ, Drews A, Loch S, Mohr F, Philipp SE, Lambert S *et al*. (2010). TRPM3 channels provide a regulated influx pathway for zinc in pancreatic beta cells. Pflugers Arch 460: 755–765.

Wang L, Ma W, Zhu L, Ye D, Li Y, Liu S *et al*. (2012). ClC-3 is a candidate of the channel proteins mediating acid-activated chloride currents in nasopharyngeal carcinoma cells. Am J Physiol Cell Physiol 303: C14–C23.

Zifarelli G, Pusch M (2007). CLC chloride channels and transporters: a biophysical and physiological perspective. Rev Physiol Biochem Pharmacol 158: 23–76.

Supporting Information

Additional Supporting Information may be found in the online version of this article at the publisher's web-site:

http://dx.doi.org/10.1111/bph.12521

Table S1 List of all 1,4-dihydropyridine derivatives used in this study together with their chemical structures.
Table S2 List of all steroidal compounds used in this study together with their chemical structures.
Table S3 Listing of the numerical values used to draw the bar plots of the various figures in this paper.
Figure S1 Stably transfected myc-tagged mouse TRPM3 is expressed in HEK cells even at high passage numbers. Untransfected HEK293 cells (control) and HEK293 cells stably transfected with myc-TRPM3 (passage number 23) were solubilized as described (Behrendt *et al*., 2009) and equal amounts of protein were loaded on 6% and 12% slab gels. Subsequently, SDS-PAGE and Western blotting were performed according to standard procedures. Nitrocellulose membranes were incubated with either (A) anti-Akt (Cell Signalling #9272, 1:500) or (B) anti-c-myc (Roche, clone 9E10, 1:500) antibodies. Blots were visualized by utilizing IRDye® 800CW labelled secondary antibodies and the ODYSSEY® Sa infrared imaging system (LI-COR Biosciences).
Figure S2 Current-voltage relationships of the recordings presented in Figure 1B (A), Figure 2C (B), Figure 4A (C), Figure 5A (D), Figure 5D (E), Figure 6D (F) and Figure 7B (G).
Figure S3 The effects of methyl-β-cyclodextrin and cholesterol on the activity of mouse TRPM3 channels. Ca^{2+} imaging experiments during the application of 100 μM PS on TRPM3 expressing cells (stably transfected) that were untreated controls (black trace) or pretreated with a cholesterol: methyl-β-cyclodextrin complex (at a concentration ratio of 1:5 mM) at 37°C for 1 h during Fura2 loading (blue trace) or methyl-β-cyclodextrin (2.78 mM) alone (red trace). Shown is the averaged response of 3 different experiments per trace (n = 203–365 in total). The differences between the experimental traces and the untreated controls were highly significant ($P < 0.001$, two-tailed unpaired Student's t-test). The results confirm the findings of Naylor *et al*. (2010), and show that also the activity of mouse TRPM3 channels is reduced by cholesterol and enhanced by the removal of cholesterol. The extracellular solution used for this experiment contained 135 mM NaCl, 5.4 mM KCl, 2 mM $CaCl_2$, 2 mM $MgCl_2$, 20 mM glucose, 10 mM HEPES, (pH 7.25 adjusted with NaOH, 315 mosmol kg^{-1}).
Figure S4 Pairwise alignment of steroidal compounds. The panels on the right side show exactly the same alignment but rotated by approximately 90°. (A) Comparison of PS with epiallopregnanolone sulphate (3β,5α). (B) Comparison of PS with epipregnanolone sulphate (3β,5β). (C) Comparison of PS with pregnanolone sulphate (3α,5β). (D) Comparison of PS (*nat*-PS, 3β) with *ent*-PS (3α). (E) The same comparison of PS (*nat*-PS, 3β) with *ent*-PS (3α), but *ent*-PS was flipped by 180° along its long axis (extending approximately from C3 to C17). Note that the sulphate moiety at the C3 position can rotate rather freely in all substances. Its position is therefore not the focus of these comparisons. The alignments were generated by manually selecting pairs of atoms to align. For panels B and C, the carbon atoms of the C and D ring, together with C20 were used. For panels A and D, carbon atoms throughout the steroid backbone were used (and C20 for A). For aligning the flipped *ent*-PS (E), the sulphur and the oxygen atom attached to C3, C3, C9 and C10 were selected.